ISSN 2349-4506
Impact Factor: 2.785

Global Journal of Engineering Science and Research Management

NUMERICAL MODELING VALIDATION OF REINFORCED CONCRETE SLABS UNDER HIGH-MASS LOW-VELOCITY IMPACT USING ANSYS WORKBENCH EXPLICIT DYNAMICS SYSTEM

Waseem F. K. Al-Muqdadi (M.Sc. Student)*, Salah R. Al-Zaidee (Ph.D., Faculty Member)
* Department of Civil Engineering, College of Engineering, University of Baghdad, Republic of Iraq

DOI: 10.5281/zenodo.212377

KEYWORDS: High-Mass Low-Velocity Impact, RC Slab, Ansys Explicit Dynamics System, RHT Concrete Damage Model, Cowper-Symonds Strength Model.

ABSTRACT
An investigation into the reinforced concrete slab behavior under impact with different parameters including slab thickness, longitudinal reinforcement ratio, and transverse reinforcement ratio has been conducted and presented in this study. The main focus of the work is to study the local and global response of reinforced concrete slabs under high-mass, low-velocity impacts dynamic loading. ANSYS Workbench V.17.0 commercial software has been used in the numerical modeling and simulation of the dynamic problem using the Explicit Dynamics System. The constitutive modeling adopted the RHT Concrete Damage Model for the concrete material and the Cowper-Symonds Strength for the steel reinforcement bars. The steel impactor, the loading plate, and the steel supports were modeled as rigid bodies during the simulation. The analyses results were compared with that of the experimental tests conducted by another researcher [1] which have been described in detail. The validity of the proposed numerical model has been demonstrated by conducting a comparison of the analysis results with the experimental tests where it has been concluded that the presented numerical model is capable of predicting the peak value of the impact force-time history, peak displacement-time history, and showed an acceptable crack pattern and damage criteria similar to that of the tests. Based upon this investigation findings, a conclusion is made that the ANSYS Workbench Explicit Dynamics and the RHT Concrete Damage model afford powerful and reliable results to simulate the impact problem of high-mass low-velocity falling weights on reinforced concrete slabs, in spite of its simple input and few parameters relative requirements.

INTRODUCTION
The impact phenomenon physics is essentially involving momentum and energy conservation. When a structure is stroke by a moving object, the force which causes deceleration of the mass fulfills momentum conservation. The impacting body kinetic energy will be transformed partially to strain energy within the target and dissipated partially through local plastic deformation and friction in addition to radiation of the strain energy away in the form of stress waves. Predicting the details are very challenging, but few simple estimations based on first principles of dynamics typically can lead to sensible response estimations.

The main problem most often is involving deformability estimate. A rigid impact hypothesis is useless in general, since rigidity denotes an immediate change in velocity, thus lead to an infinite acceleration and force. The deceleration is limited in real structures by deformations in both elastic and plastic, which in turn mitigates the blow, besides a rational estimation of the stiffness or local compliance at the impact point is made.

In case of impact being a circumstance of routine service, a real dynamic analysis is required where the structure should be or nearly remain elastic. In the design of many mechanical or structural problems, provision of an evidence is required to keep a substantial intact structure, even when damaged. In the provision of a nearly elastic global response the local plastic deformation may be allowed. The effect of St Venant *(Saint-Venant's principle states that high order momentum of mechanical load (moment with order higher than torque)* decays so fast that they never need to be considered for regions far from the short boundary) allows a separate consideration of the local effects as a first rough calculation. Energy equivalence based methods are useful in both behavior, elastic and plastic.

ISSN 2349-4506
Impact Factor: 2.785

Global Journal of Engineering Science and Research Management

REVIEW OF LITERATURE

The main consideration for examining a structure when subjected to an impact is to look for local damage including penetration, scabbing, perforation, and/or punching shear, as well as the global structural response in consideration of flexural and shear capacities, global damage, etc. The definition of the local effects are as explained below.

Penetration (x_p) : the development of the crater depth in the target at the impact zone.
Perforation (t_p) : complete target penetration by the impactor with and without exit velocity.
Scabbing (t_{sc}) : the target material ejection from the opposite of the impact face.
Spalling (t_{sp}) : the target material ejection from the impacted face.

Figure 1, *Figure 2*, *Figure 3*, and *Figure 4* show the above local effects as well as the overall response phenomena.

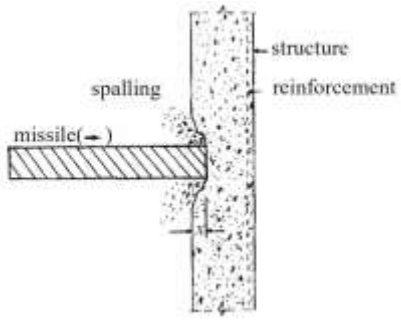

Figure 1: Local effect of penetration (x) and spalling

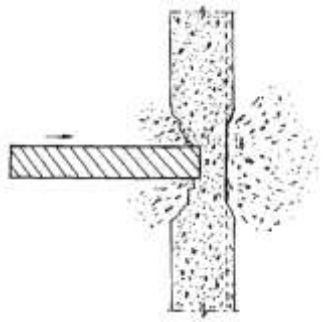

Figure 2: Local effect of scabbing

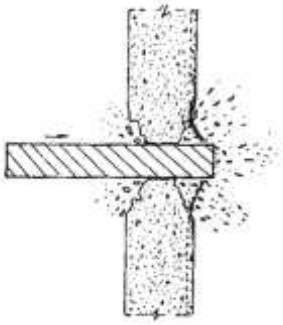

Figure 3: Local effect of perforation

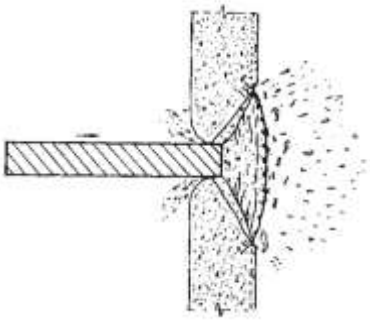

Figure 4: Local effect of a punch type shear failure

Criteria for point (i) involves the transient stress state complex nature. Many empirical formulas to predict penetration of concrete elements caused by missile impacts have been developed so far which are dependent on the availability of experimental data. These formulas remain true for smaller missiles which are partially deformable after being impacted. Besides these are the undeformable and deformable missiles interaction problems. The deformability of the missile prolongs the impact duration and similarly reduces the depth of penetration x_p, however, it has minor effect on thicknesses of scabbing and perforation. It is out of the scope of this study to elaborate more on the development of these formulas.

Apart from the empirical formulas developed to predict penetration depth of concrete elements subject to missile impacts (both deformable and non-deformable), requirement of further comprehensive nonlinear analyses to consider mechanisms of instantaneous formed failure, interaction of the impactor with the structure or target, nonlinear effects of material and geometry, and to evaluate the global damage to both the structures and impactors. This is considered as part of this study using Finite Elements method of analysis to model the free-fall impact problem on concrete slabs using ANSYS Workbench Explicit Dynamics System, a commercial finite element analysis software, including concrete nonlinear material modeling with geometric nonlinearity, and effect of different boundary conditions.

Several researchers have worked on conducting experimental tests to investigate the impact phenomenon on the behavior of reinforced concrete slabs. A similar example is the series of experimental tests conducted by Xiao, Li [1] involving high-mass low-velocity falling weight impact on reinforced concrete slabs with different parameters including slab thickness, longitudinal reinforcement ratio, and transverse reinforcement ratio. Other researchers worked on the development of numerical models using different modeling techniques available in the commercial finite elements software including different material models for the constitutive modeling of concrete and steel reinforcing bars such as the work done by Sangi [2] who developed a numerical model using the commercial LS-DYNA software to perform three-dimensional finite element modeling of different configurations of reinforced concrete slabs under high-mass low-velocity impacts and compared the numerical modeling results with the test results of similar slab experiments conducted at Heriot-Watt University for validation of the proposed numerical models.

The primary objective of this research is to develop a numerical model for use by ANSYS Workbench Explicit Dynamics System, to simulate the behavior of reinforced concrete slabs under high-mass low-velocity impact, using the RHT Concrete Damage model developed by [Riedel, Thoma [3], 4, 5] for the constitutive modeling of concrete material and the Cowper-Symonds Strength model [6, 7] for the modeling of steel reinforcing bars and compare the numerical results with those obtained by the tests of the slab specimens of the experiments conducted by Xiao, Li [1] for validation of the proposed model.

NUMERICAL MODELING AND ANALYSIS

Introduction

This study involves the high-mass, low velocity impact analysis of reinforced concrete slabs. Numerical modeling and analysis has been performed on reinforced concrete slabs under impact loading that were tested by Xiao, Li [1] and conclusions on the validation of the model has been described.

During this experimental work, manufacturing and testing of eighteen reinforced concrete slabs subject to static (0.0004 m/s), medium (0.4 m/s) and high (2 m/s) concentrated loading rates at center of slab has been conducted by Xiao, Li [1] using a displacement controlled rapid loading machine. The experimental data were used to study the influence of different loading rates as well as other parameters including slab depth, longitudinal and transverse reinforcement ratios on the reinforced concrete slabs performance. In addition, manufacturing and testing of another six slabs subject to low velocity (5.425 m/s) impact has been conducted using a drop weight machine. The high loading rate obtained results when compared with that of the impact tests showed similarity in the damage process, mode of failure, energy absorption capacity, and strain rate effects. Good correlation has been obtained of the high loading rate test with the impact test that suggested the prospect of implementing high loading rate test to assist in understanding the performance of the slab subject to low velocity impact.

In this study, the slab specimens tested by Xiao, Li [1] under low-velocity impact are numerically modeled and analyzed, and a comparison of numerical results and experimental results is conducted to validate the numerical model as explained in the following sections.

Description of Slab Tests

For a more comprehensive description of the slab tests including slab specimens, experimental procedure and test setup, instrumentation, as well as description of the test results including crack patterns and damage, absorbed energy, strain and corresponding strain rate, and impact force and inertial effect can be found as detailed by the work of Xiao, Li [1].

Finite Element Modeling

The impact tests conducted on the slab specimens by Xiao, Li [1] have been numerically modeled and analyzed using ANSYS Explicit Dynamics. A three-dimensional finite element model has been created for the entire slab with the use of the Explicit Dynamics Lagrangian formulation. The simulation has been done using a workstation computer with a Windows operating system, which assisted in reducing the solution running times to a convenient level. The detailed modeling steps are described in the following sections.

ISSN 2349-4506
Impact Factor: 2.785

Global Journal of Engineering Science and Research Management

Geometry

The ANSYS Workbench DesignModeler, which provides analysis-specific geometry modeling tools, has been used to model the different type of objects of the problem. The concrete slabs with dimensions of 1200 × 1200 × 100 mm and 1200 × 1200 × 150 mm have been modeled using the hexahedron solid body. The loading circular steel plate with 200 mm diameter has been modeled using a cylindrical solid body with an assumed thickness of 20 mm and placed in the center of the tested slab contacting the top face of the slab solid body. The steel supporting plates with 100 mm in width and 980 mm in length have been modeled using hexahedron solid bodies with an assumed thickness of 20 mm and were placed to match their corresponding locations as shown in Figure 5 reducing the slab clear span to 1000 mm. The 500 kg drop hammer with 200 mm diameter flat nose used to impact the center of the slab specimen has been modeled using a cylindrical solid body with a calculated height of 2030 mm in order to produce a volume that is equivalent to the hammer weight using a steel density of 7800 kg/m3, and was placed in the center of the tested slab contacting the top face of the circular loading plate solid body. The reinforcement bars have been modeled using discrete line body objects and were placed in exact coordinates matching their respective locations as of Figure 6 with circular cross-sections matching their corresponding diameter as explained in Table 1 and Table 2.

a. Rapid loading machine b. Drop weight system c. Supporting system

Figure 5: Test setup of the slab specimens tested by Xiao, Li [1]

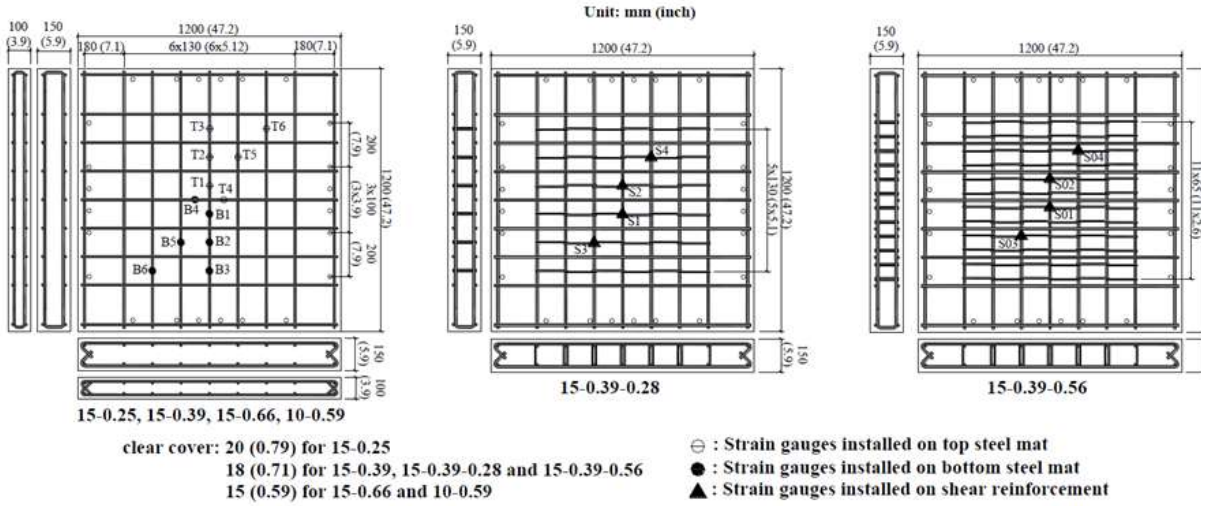

Figure 6: Reinforcement layout of slab specimens tested by Xiao, Li [1]

ISSN 2349-4506
Impact Factor: 2.785
Global Journal of Engineering Science and Research Management

Table 1: Summary of slab specimens tested by Xiao, Li [1]

Specimen	Slab thickness, mm	Compressive strength of concrete, MPa	Longitudinal reinforcement	Shear reinforcement	Flexure capacity, kN	Shear capacity, kN	Expected failure mode	Observed failure mode
I-10-0.59	100	42.9	T10	-	161	140	Shear	Shear
I-15-0.25	150	42.9	T8	-	134	266	Flexure	Shear
I-15-0.39	150	45.0	T10	-	268	266	Shear	Shear
I-15-0.66	150	42.9	T13	-	462	266	Shear	Shear
I-15-0.39-0.14	150	42.3	T10	R6	268	326	Flexure	Shear
I-15-0.39-0.28	150	42.3	T10	R6	268	416	Flexure	Shear

Table 2: Properties of reinforcing bars of slab specimens tested by Xiao, Li [1]

Rebar	Diameter, mm	Yield strength, MPa	Ultimate strength, MPa
T8	8	443	504
T10	10	576	655
T13	13	605	690
R6	13	282	392

It should be noted that the thicknesses of the loading plate and steel supports were not provided in the specimen description by Xiao, Li [1], however, this does not affect the modeling as far as these bodies will be modeled as rigid body solid elements.

The created geometry model for the whole problem using ANSYS DesignModeler is illustrated in Figure 7. This model is then imported by the Explicit Dynamics system to continue with the modeling and analysis steps.

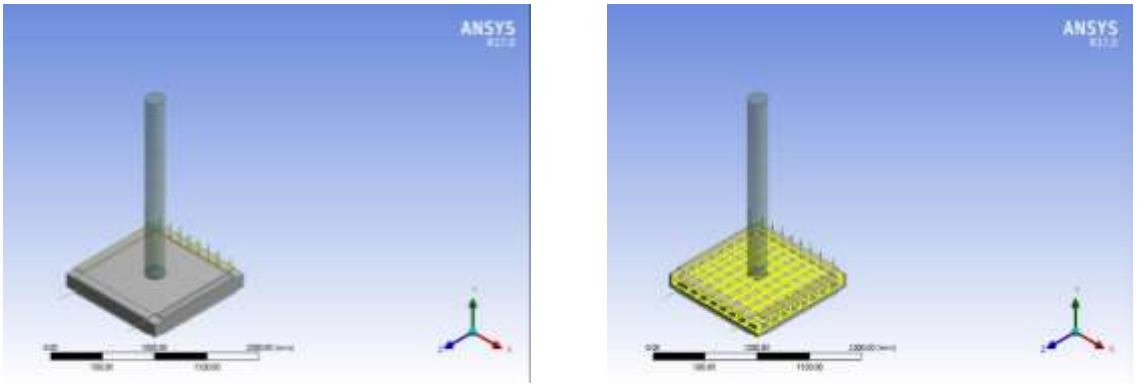

a. Geometry model of the whole solid bodies.

b. Geometry model of the reinforcement discrete line bodies embedded within the concrete slab solid body.

Figure 7: Geometry model of the slab specimens under impact tested by Xiao, Li [1] modeled using ANSYS Workbench DesignModeler

Material and Engineering Properties

ANSYS Explicit Dynamics provides multiple material models for concrete and reinforcement modeling. In the present study, the RHT Concrete Strength model has been adopted to model the concrete slabs material. The concrete material properties that is used in the slab simulations are given in

ISSN 2349-4506
Impact Factor: 2.785
Global Journal of Engineering Science and Research Management

Table ***3***. The Cowper-Symonds Strength model has been adopted to model the reinforcement material with the properties as shown in
Table ***4***. The steel circular loading plate, steel supports and steel impactor were modeled as rigid bodies with a density of 7800 kg/m^3 with an elastic modulus of 210 GPa, and a Possion's ratio of 0.30.

Table 3: Material properties of concrete used as input data for the RHT Concrete model within ANSYS Engineering Data library

Name	Symbol	Units	Value(s)
Density		kg/m^3	2314 (default)
Poisson's Ratio	ν	None	0.19
Compressive Strength	f_c	MPa	42.3, 42.9, or 45.0
Tensile to Compressive Strength	f_t/f_c	None	0.1 (default)
Shear to Compressive Strength	f_s/f_c	None	0.18 (default)
Intact failure surface constant *A*	A_{FAIL}	None	1.6 (default)
Intact failure surface exponent *N*	N_{FAIL}	None	0.61 (default)
Tens./Comp. Meridian ratio	$Q_{2.0}$	None	0.6805 (default)
Brittle to Ductile Transition	BQ	None	0.0105 (default)
Hardening Slope		None	2 (default)
Elastic Strength/ft		None	0.7 (default)
Elastic Strength/fc		None	0.53 (default)
Fracture Strength Constant	B	None	1.6 (default)
Fracture Strength Exponent	m	None	0.61 (default)
Compressive strain rate exponent	α	None	0.032 (default)
Tensile strain rate exponent	δ	None	0.036 (default)
Maximum fracture strength ratio	$SFMAX$	None	1E+20 (default)
Use cap on elastic surface		None	Yes (default)
Damage constant D1	D_1	None	0.04 (default)
Damage constant D2	D_2	None	1 (default)
Minimum strain to failure		None	0.01 (default)
Residual Shear modulus fraction		None	0.13 (default)

Note: The default values of the RHT Concrete model within the Engineering Data library has been derived and tested for concrete strength of 35MPa and are kept the same in this study. Only values of concrete compressive strength need to be changed based on the slab specimen selected for modeling and analysis.

Table 4: Material properties of steel reinforcement used as input data for the Cowper-Symonds Strength model within ANSYS Engineering Data library

Name	Symbol	Units	Value(s)
Density		kg/m^3	7850 (default)
Poisson's Ratio	ν	None	0.3 (default)
Tensile Yield Strength	f_y	MPa	443, 576, 605, or 282
Elastic Modulus	E_{el}	GPa	200 (default)
Tangent Modulus	E_t	GPa	19 (default)

Note: The default values of the Cowper-Symonds Strength model within the Engineering Data library has been used and kept the same in this study. Only values of steel yield strength need to be changed based on the reinforcement type selected for modeling and analysis.

Defining Parts Behaviors

Once the geometry model has been imported by the Explicit Dynamics system, the "Parts Behaviors" need to be defined for all model bodies. This will associate the stiffness behavior of those parts to either a "Flexible Body" or a "Rigid Body". The Flexible Body property will assign a stiffness matrix for that body in the solver, while the Rigid Body essentially reduces the representation of the part to a single point mass thus significantly reducing the solution time. Definition of a body's stiffness behavior as "Rigid", it means that the application will not allow

the body to deform during the solution process, it will not mesh the rigid body, and the solver represents the body as a single mass element. However, the system maintains the element's mass and inertial properties.
Consequently, the concrete slab solid is scoped as a Flexible Body while the steel circular loading plate, steel supports and the steel drop-weight (impactor) are scoped as "Rigid Bodies". Reinforcement line bodies will remain as discrete flexible elements.

Defining the Reference Frame
The Reference Frame determines the analysis treatment perspective of the body for an Explicit Dynamics analysis. The Reference Frame property is available for solid bodies when an Explicit Dynamics system is part of the solution. The valid values are Langrangian (default) and Eulerian (Virtual). Eulerian is not a valid selection if Stiffness Behavior is set to Rigid.

Consequently, the Reference Frame is set to Lagrangian formulation for all bodies of the problem in this study to be analyzed in the Explicit Dynamics system.

Material Assignment
Once the geometry is imported by the Explicit Dynamics system, the material for the simulation already defined in the Material and Engineering Properties section is assigned to each respective geometry body as explained earlier. The nonlinear material effects of the defined material properties are selected and the program will use all applicable material properties including nonlinear properties such as stress-strain curve data and failure criteria.

Defining Connections and Body Interactions
Once the material properties and part behavior of the model are addressed, body interaction of the bodies in the model need to be applied so that they are interacted together in sustaining the applied loads for analysis.

Trajectory contact detection algorithm with the Penalty formulation has been assigned for all scoped body interactions of the model. The Body Self Contact and Element Self Contact properties were set to Program Controlled for all bodies scoped in the Body Interactions. Table 5 illustrates the Body Interactions matrix applied in the current model.

Table 5: Body Interactions matrix applied on the scoped bodies of the geometry model

Scoped Bodies of the Geometry Model	**Interaction Type**	**Description of Body Interactions Simulation Event**
Body Interactions 1		
One (1) concrete slab solid body plus eight (8) steel supporting plates	Bonded type with a contact detection tolerance of 1E-4 mm and "Not Breakable" bond definition selection	This unbreakable bond contact is used to simulate the fixation between the steel support plates at the top and bottom face edges of the slab specimens and the concrete slab
Body Interactions 2		
Twenty seven (27) steel reinforcement line bodies, one (1) steel circular loading plate solid body, and one (1) cylindrical steel impactor solid body	Frictionless type	This frictionless type contact is used to simulate the interaction between the steel impactor, steel loading plate, and the steel reinforcement once they become in contact during impact loading time history. This frictionless contact is automatically detected as surface to surface contact and surface to line contact formulation
Body Interactions 3		
All bodies (38 bodies)	Reinforcement type	This reinforcement body interaction type is used to apply discrete reinforcement to solid bodies. All line bodies scoped to the object will be flagged as potential discrete

Scoped Bodies of the Geometry Model	Interaction Type	Description of Body Interactions Simulation Event
		reinforcing bodies in the solver. On initialization of the solver, all elements of the line bodies scoped to the object which are contained within any solid body in the model will be converted to discrete reinforcement. Elements which lie outside all volume bodies will remain as standard line body elements
Body Interactions 4		
One (1) concrete slab solid body plus twenty seven (27) steel reinforcement line bodies	Bonded type with a contact detection tolerance of 1E-4 mm and "Breakable" bond definition selection with penalty Stress Criteria. Normal stress limit of 7.5 MPa and a normal stress exponent of 1 is entered. Shear stress limit of 7.5 MPa and a shear stress exponent of 1 is entered	Bonded type body interaction can be used to model bond-slip between reinforcement bars and the surrounding concrete by enabling the "Breakable Bond" option and specifying a "Stress Criteria" as a condition to break (or release) the bond once reached during the analysis. The stress criteria for the bond-slip between steel reinforcement and concrete was selected based on experimental results conducted by Fu and Chung [8]
Body Interactions 5		
One (1) concrete slab solid body, one (1) steel circular loading plate solid body, and one (1) cylindrical steel impactor solid body	Frictionless type	This frictionless type contact is used to simulate the interaction between the steel impactor, steel loading plate, and the concrete slab once they become in contact during impact loading time history. This frictionless contact is automatically detected as surface to surface contact formulation

Meshing and Finite Element Discretization

The meshing process is defined as the spatial discretization of the geometry into nodes and elements. Both meshing accompanied with material properties form the mathematical representation of the structure stiffness and mass distribution.

The meshing of the model is done automatically at solving time. The determination of the default element size is done according to multiple factors that include the size of the overall model, the proximity of other topologies, curvature of the body, and the feature complexity. Adjustment of the mesh fineness up to four times, and eight times for an assembly, is done when there is a necessity for the achievement of a successful mesh. Mesh controls are used to assist in fine tuning the mesh to a more accurate analysis.

In the current model, the concrete slab solid body and steel supporting plate solid bodies have been discretized with eight-noded hexahedron elements. The aspect ratio of concrete slab elements is (1) one. The minimum element size is chosen to be 10 mm for the concrete slab and 20 mm for the steel circular loading plate, steel supporting plates and steel impactor. Spatial discretization of the reinforcement bars was done using beam elements. As an example, the finite element mesh for (I-15-0.66) slab specimen is shown in Figure 8. Total number of nodes is (286240) and total number of elements is (256318).

ISSN 2349-4506
Impact Factor: 2.785
Global Journal of Engineering Science and Research Management

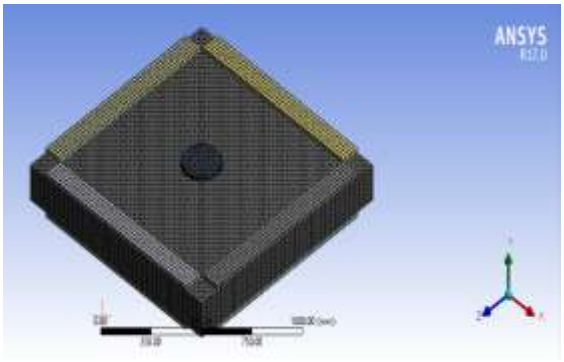

a. Meshing of the concrete slab (10 mm hexahedron element size), steel supporting plates (20 mm hexahedron element size) and steel circular loading plate (20 mm hexahedron element size).

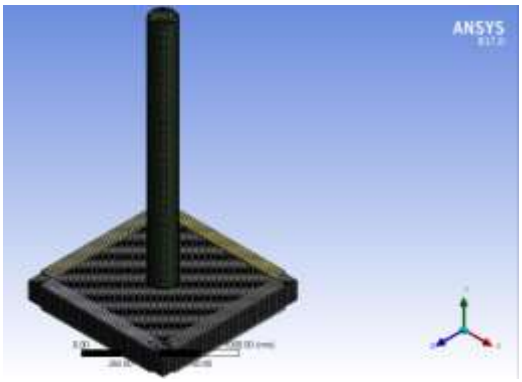

b. Meshing of the whole model including the steel impactor.

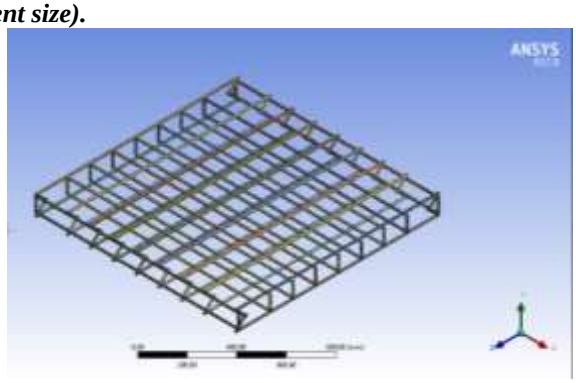

c. Meshing of the steel reinforcement with 10 mm discrete beam elements.

Figure 8: Finite element mesh of the (I-15-0.66) slab specimen under impact tested by Xiao, Li [1]

Configuring Analysis Settings

The input values of the basic Analysis Settings controls of the Explicit Dynamics analysis of the current study are shown in Figure 9.

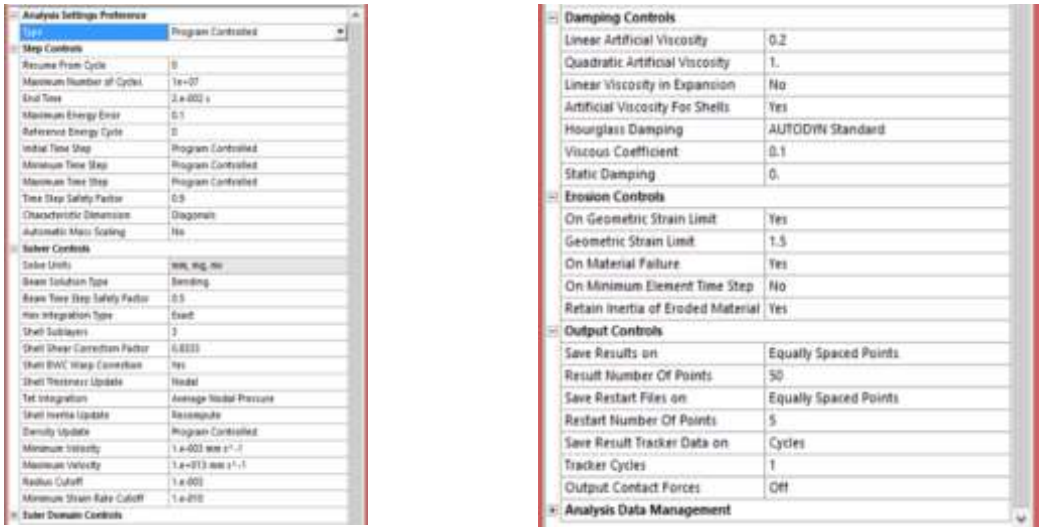

Figure 9: Input values of the Analysis Settings controls of the impact problem in Explicit Dynamics system

It should be noted from the above figure the following:

1. The End Time value of the Step Controls is entered as 2E-02 s (i.e. 20 ms); however, this could be increased to 40 ms to allow for more time history simulation but this will increase solver time duration.
2. The Time Step controls value is set to Program Controlled to allow for automatic calculation of the time step by the solver.
3. The Hourglass Damping was set to AUTODYN Standard to allow the solver to automatically control the hourglass damping values and damping format.
4. The Erosion Controls is enabled on Geometric Strain Limits and set to 150%, in addition to Material Failure. The inertia of the eroded material is retained during the solution.

Defining Initial Conditions

For the impact problem being considered in the current case study; the free-fall 500 kg mass impactor should impact the steel circular loading plate, which in turn will transfer the impact force to the concrete slab specimen, from a falling height of 1.5 m. The velocity at time of impact is calculated to be 5.425 m/s. As simulation of the impact problem is commencing once the impactor hits the circular loading plate and progresses until the specified End Time provided, the impact velocity is considered an initial condition to the problem and is scoped to the steel impactor solid object as shown in Figure 10.

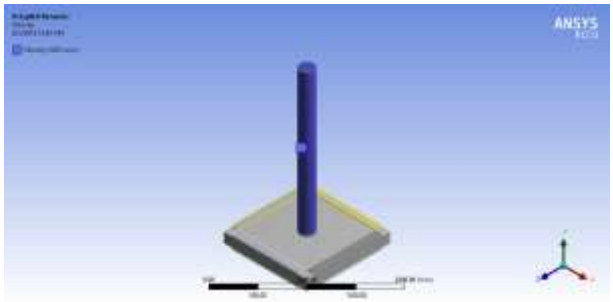

Figure 10: Defining the impact velocity of 5.425 m/s as an initial condition and scoping this condition to the steel impactor in Explicit Dynamics system

Applying Boundary Conditions (Loads and Supports)

The following boundary conditions have been applied for the model considered in this case study:

Standard Earth Gravity

This is an inertial type boundary condition that simulates gravitational effects on a body in the form of an external force. Gravity is a specific example of acceleration with an opposite sign convention and a fixed magnitude. Gravity loads cause a body to move in the direction of gravity. By virtue of Standard Earth Gravity's physical characteristics, this boundary condition is always applied to all bodies of a model. Standard Earth Gravity is constant, and the direction is assigned to y-axis of the global coordinate system in the negative direction as shown in Figure 11.

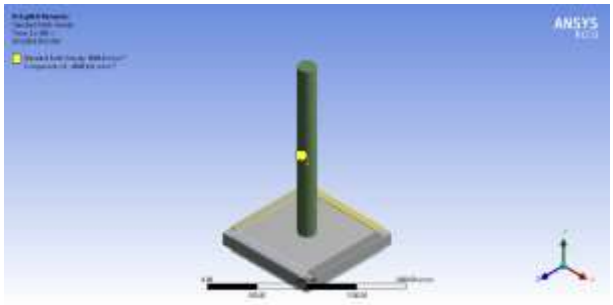

Figure 11: Applying the Standard Earth Gravity as an inertial type boundary condition that is scoped to all model bodies in the Explicit Dynamics system

Fixed Supports

This is a support type boundary condition that prevents one or more of the following:

1. Flat or curved faces from moving or deforming;
2. Straight or curved edges from moving or deforming; and
3. Vertices from moving.

This boundary condition is applied to all eight (8) steel supporting plate bodies in the model to provide fixation to the concrete slab body as shown in Figure 12.

Figure 12: Applying the Fixed Supports as a support type boundary condition that is scoped to the eight (8) steel supporting plate bodies of the model in the Explicit Dynamics system

Mesh Sensitivity

For studying the element mesh sizes whether it affects the analysis or not, the slabs have been modeled using three different mesh sizes of 10 mm, 15 mm, and 20 mm respectively. Table 6 shows the details of the mesh data for the current slab model. For each slab, refined element mesh sizes have been used to carry out the analysis and a comparison of results has been conducted to see if there is any variance in the acceleration-, impact force- and displacement-time histories of selected areas of the slab.

Table 6: Mesh size data for slab (I-15-0.66) model

	Mesh 1	Mesh 2	Mesh 3
Nodes	234256	72171	33489
Solid elements	216000	64000	28800
Beam elements	4662	3132	2358
Element size	10 × 10 × 10 mm for solid elements, 10 mm for beam elements	15 × 15 × 15 mm for solid elements, 15 mm for beam elements	20 × 20 × 20 mm for solid elements, 20 mm for beam elements

Acceleration-time histories of the top slab surface obtained from the analysis of the above mentioned three mesh sizes for slab (I-15-0.66) specimen are shown in Figure 13.

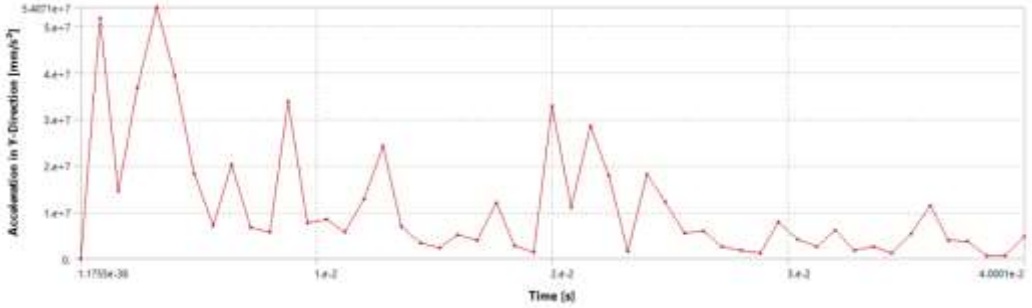

a. Acceleration time history of the top slab surface obtained from a slab model of 20 mm mesh size.

ISSN 2349-4506
Impact Factor: 2.785

Global Journal of Engineering Science and Research Management

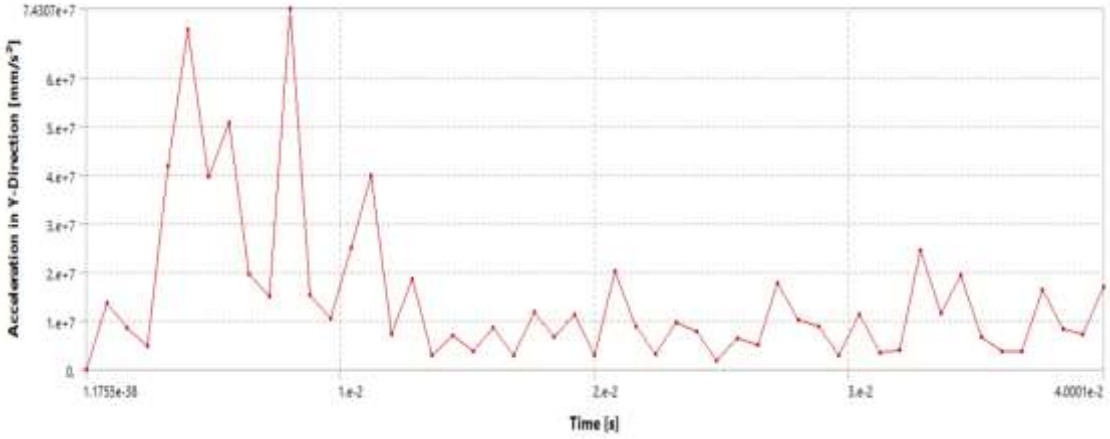

b. Acceleration time history of the top slab surface obtained from a slab model of 15 mm mesh size.

c.

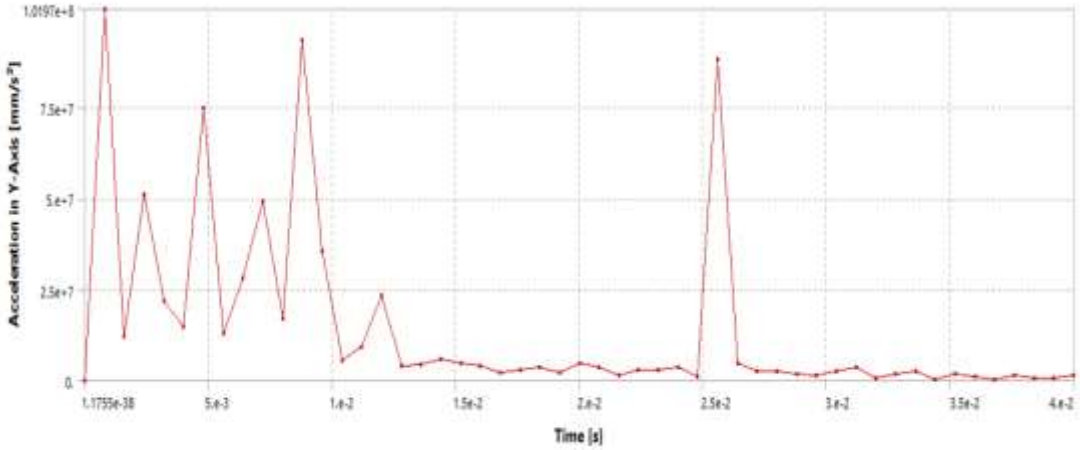

d. Acceleration time history of the top slab surface obtained from a slab model of 10 mm mesh size.

Figure 13: Comparison of acceleration time histories of the top slab surface obtained from the analysis for three different mesh sizes of slab (I-15-0.66)

The above acceleration curves show similar shape for the three mesh sizes for slab (I-15-0.66) specimen but with a slight difference in the magnitude of the peak acceleration. Also, it can be observed that a more damped oscillation with the refined mesh compared to the coarser mesh is resulted from the analysis. This could be attributed to the size of discrete particles, where the finer the particles (finer mesh) the more accurate simulation of acceleration wave propagation is resulted narrowing down the impact effect to be under the region of the impact zone.

Figure 14 shows the impact force-time history of the slab (I-15-0.66) specimen resulted from the analysis using the above mentioned three mesh sizes which are all compared to the tested impact force-time history. It is clearly shown that the magnitude of the peak impact force of the three mesh sizes are very close to that of the experimental test. However, a more damped oscillation of the impact force just after the impact period is passed can only be observed in the analysis results using the finer mesh of 10 mm and shows a similar shape to that resulted from the experimental test. This also could be attributed to the size of the discrete particles as explained above.

The indication is that performing the analysis with the 20 mm coarse mesh can be considered close with that of the 10 mm and 15 mm refined meshes in terms of the magnitude of the peak impact force but a more accurate shape of the time history event is obtained using the refined 10 mm mesh.

ISSN 2349-4506
Impact Factor: 2.785
Global Journal of Engineering Science and Research Management

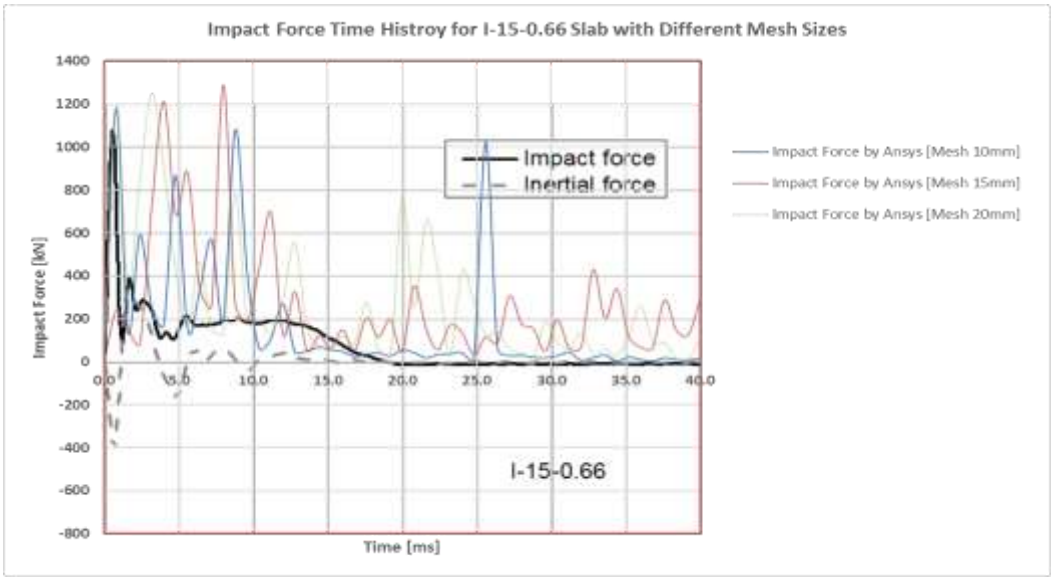

Figure 14: Comparison of impact force-time histories obtained from the analysis for three different mesh sizes of slab (I-15-0.66) with that resulted from the experimental tests conducted by Xiao, Li [1]

Graphs of transient displacement-time histories resulted from the analysis of slab (I-15-0.66) specimen using the above mentioned mesh sizes have been compared and are shown in Figure 15. For mesh sizes of 10 mm, 15 mm, and 20 mm, the peak displacements at the location of sensor D2 are 0.32 mm, 0.413 mm, and 0.814 mm respectively. It can be considered that a close agreement of the peak values for both displacements and times for the three mesh sizes are obtained. However, a more damped oscillation shape of the displacement-time history curve is resulted from the analysis using the refined mesh compared to the coarser mesh similar to the acceleration- and impact force-time histories as explained earlier. This also could be attributed to the size of the discrete particles as explained above.

The same previously described indication is that performing the analysis with the 20 mm coarse mesh can be considered close with that of the 10 mm and 15 mm refined meshes in terms of the magnitude and time of the peak displacement but a more accurate shape of the time history event is obtained using the refined 10 mm mesh.

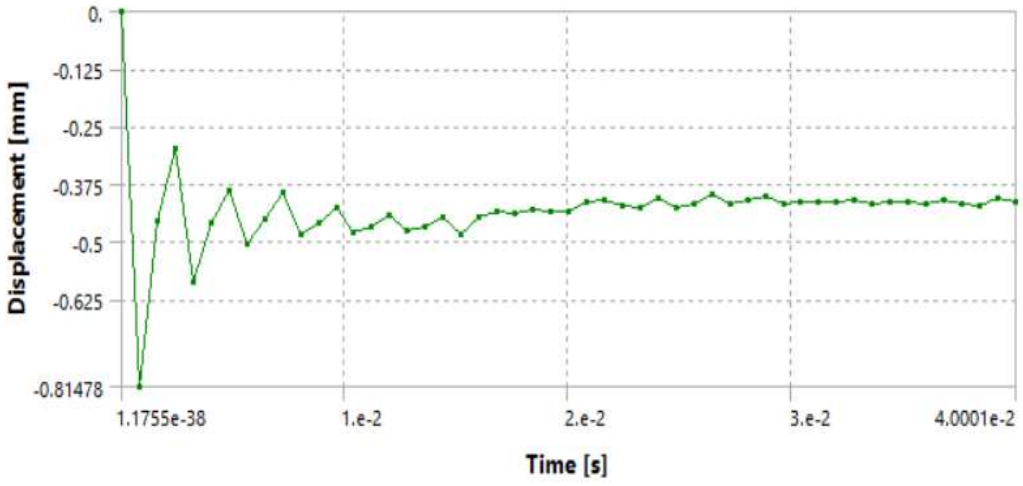

a. Transient displacement history at the location of D2 sensor obtained from a slab model of 20 mm mesh size.

ISSN 2349-4506
Impact Factor: 2.785

Global Journal of Engineering Science and Research Management

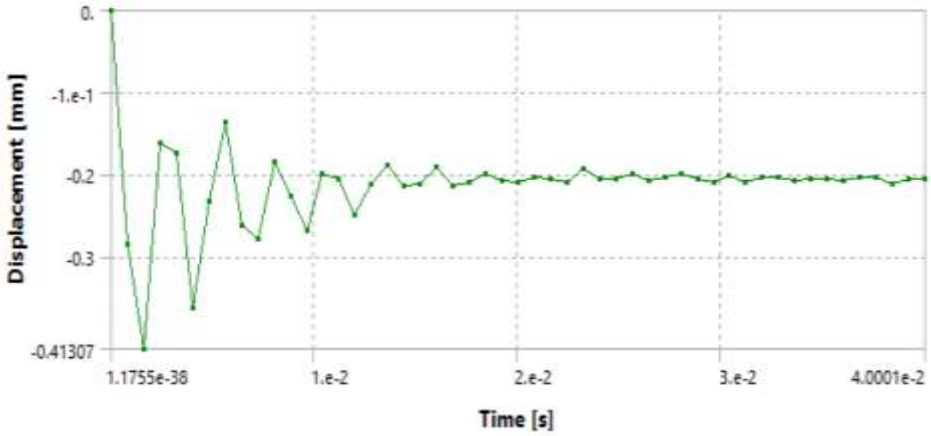

b. Transient displacement history at the location of D2 sensor obtained from a slab model of 15 mm mesh size.

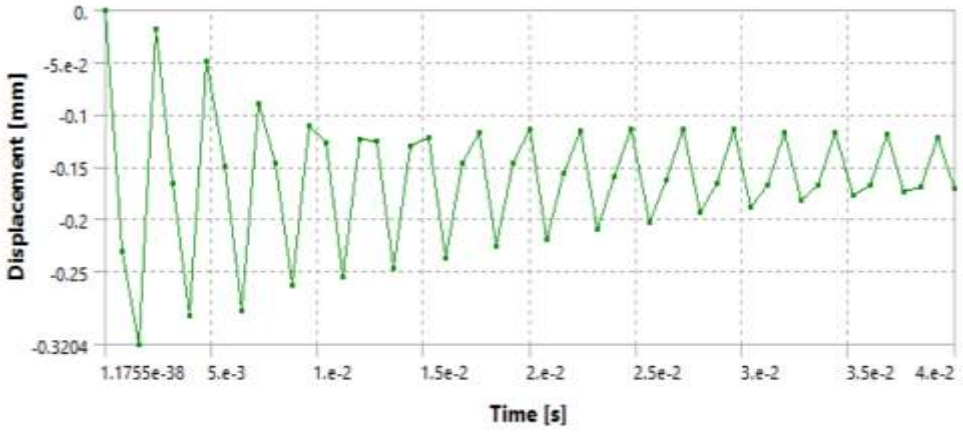

c. Transient displacement history at the location of D2 sensor obtained from a slab model of 10 mm mesh size.

Figure 15: Comparison of transient displacement histories at the location of D2 sensor obtained from the analysis for three different mesh sizes of slab (I-15-0.66)

As concluded from the above discussion, the analyses of the rest of the slab specimens using the 20 mm mesh size can be adequately considered to minimize the computational time. However, it is more preferable to use the refined 10 mm mesh to analyze the damage and crack propagation of the slab system with more refined eroded particles than the coarser mesh. This will give more accurate results but with extensive computational time. As a result the 10 mm mesh size has been adopted in the models validation of the rest of the slab specimens.

COMPARISON OF FINITE ELEMENT RESULTS AND EXPERIMENTAL RESULTS

The slab specimens considered in this study have been modeled using 10 mm mesh size. The material properties and reinforcement ratios are as described in the previous sections. A description of the results of the analyses including transient impact forces, displacement-time histories, and crack patterns and damage is elaborated in the following sections with a comparison of these results with the experimental tests of the considered slabs.

Transient Impact Forces

The transient impact force histories as obtained from the analysis are compared with the experimental tests for the considered slab specimens as illustrated in Figure 16. In general and for all slab specimens, it is shown that the peak values of the impact forces for both the analysis and the test are reached in almost a similar time at 2.0 ms

ISSN 2349-4506
Impact Factor: 2.785
Global Journal of Engineering Science and Research Management

for slab (I-10-0.59) and 1.5 ms for slabs (I-15-0.39), (I-15-0.66), (I-15-0.39-0.28), and (I-15-0.39-0.56). A lag in the time of the peak values of the impact force between the analysis (3.5 ms) and the test (2.0 ms) is observed for slab (I-15-0.25). Nevertheless, it is seen from the analysis results that the obtained force is generally larger than that of the test for all slab specimens except slab (I-15-0.25). It is also observed that the shape of the force histories shows some oscillation after passing the peak value. The stiffness of the slab-impactor interface could be the reason behind the increase of the analyses peak forces and shape function over that of the tests. Filtering and tuning of the analysis results could have been attempted for the noise reduction to reach better findings, but this could not be implemented due to the limited time frame constraint of the work.

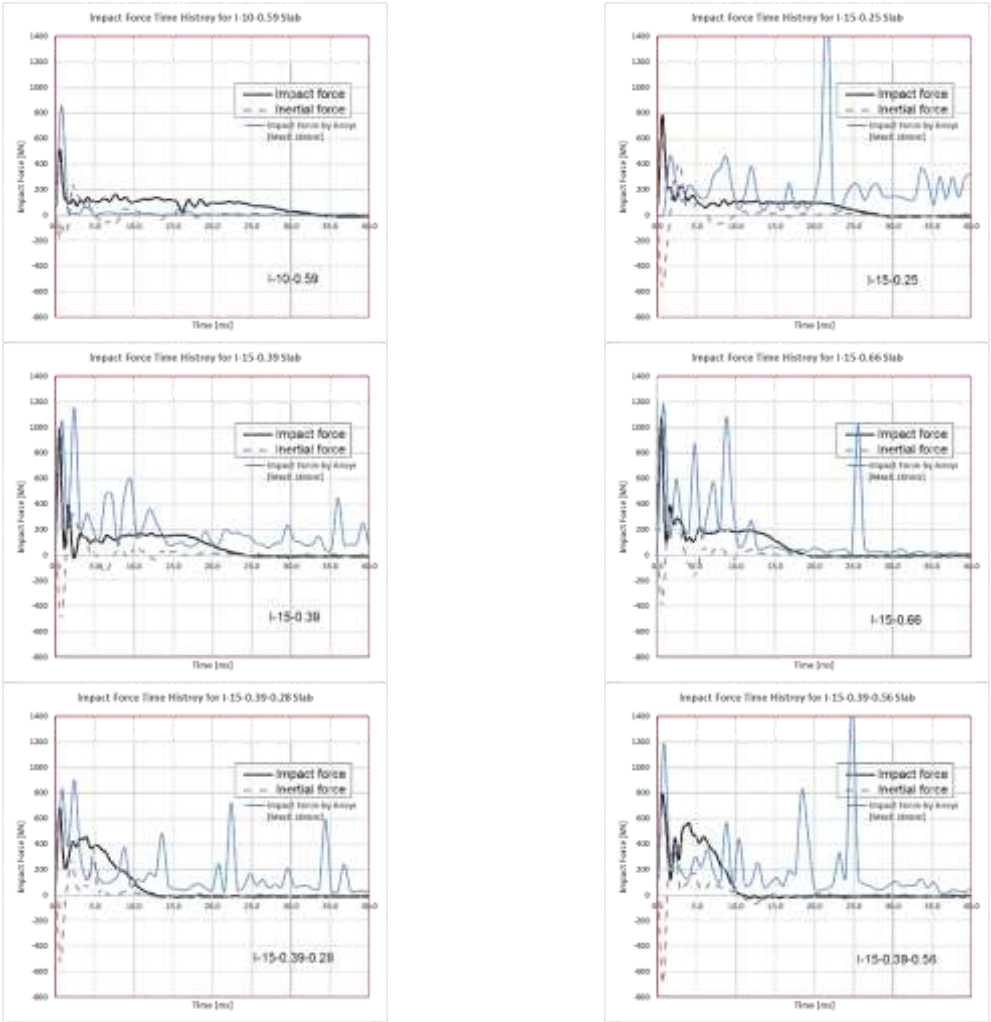

Figure 16: Recorded and simulation impact force histories for the slab specimens

Displacement Histories

The deflected shapes of (I-15-0.66) and (I-15-0.39-0.56) as obtained by the tests are shown in Figure 17 (a) and (b). Plots of the transient displacement-time histories of the analysis are obtained at the slab centers for (I-15-0.66) and (I-15-0.39-0.56) specimens and are shown in Figure 17 (c) and (d) for the purpose of demonstration of the models efficiency. The peak displacement is predicted by the analysis to be of 12.6 mm after 2.4 ms compared to 12.0 mm after 2.8 ms as obtained by the test for slab (I-15-0.66). Similarly, the peak displacement is predicted by the analysis to be of 8.3 mm after 1.6 ms compared to 21.5 mm after 5.9 ms as obtained by the test for slab (I-15-0.39-0.56).

ISSN 2349-4506
Impact Factor: 2.785
Global Journal of Engineering Science and Research Management

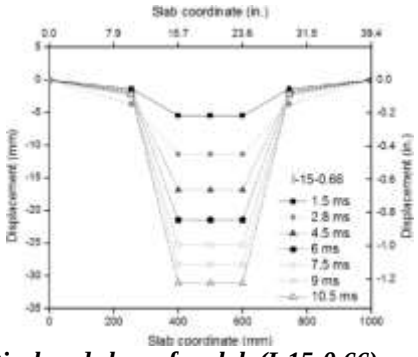

a. Displaced shape for slab (I-15-0.66) specimen as obtained by the test

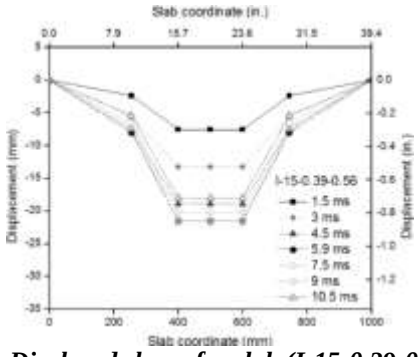

b. Displaced shape for slab (I-15-0.39-0.56) specimen as obtained by the test

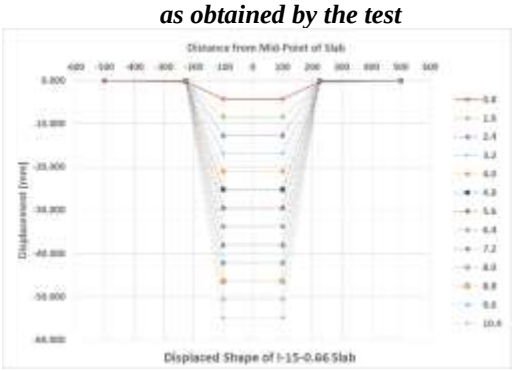

c. Displaced shape for slab (I-15-0.66) specimen as obtained by the analysis

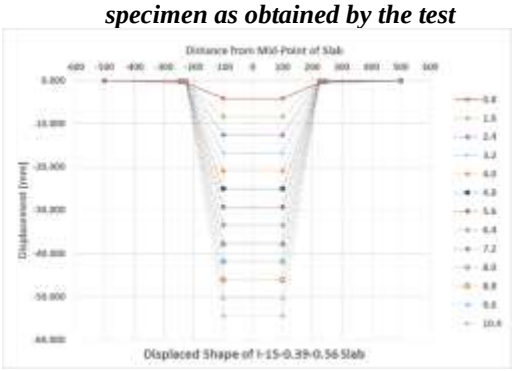

d. Displaced shape for slab (I-15-0.39-0.56) specimen as obtained by the analysis

Figure 17: Transient displacement histories as obtained from the analysis at the center of slabs (I-15-0.66) and (I-15-0.39-0.56) compared to those obtained from the tests

Crack Patterns and Damage

A comparison of the crack patterns generated from the analyses with those observed from the tests on each slab bottom faces is conducted and are shown in Figure 18. The extent of cracking and directions as well as structural damage which is caused by penetration, perforation, and scabbing can be assessed.

For all slab specimens, only slabs bottom face of each specimen could be considered for comparison due to the availability of images of only the bottom face of the slabs as provided by Xiao, Li [1]. However, it could be predicted from the analysis that the damage zone at the impact region on the top face of the slabs is of a circular penetration shape similar to the boundaries of the circular loading plate. In the case of slab specimens without shear reinforcement; i.e. slabs (I-10-0.59), (I-15-0.25), (I-15-0.39), and (I-15-0.66) specimens, the impactor fully perforated the slab specimen as demonstrated by the test, while no perforation is observed for slab specimens with shear reinforcement; i.e. slabs (I-15-0.39-0.28) and (I-15-0.39-0.56) specimens. For all slabs, the slab top face has no cracking except at the boundaries of the impactor and circular loading plate. A circular circumference cracking zone and concrete shear failure is observed at the center of the slab bottom face similar to what was observed in the test. A reasonable agreement of the damage zone diameter is shown from the analysis compared with the tests.

The analysis results are examined closely for using three mesh sizes of 10 mm, 15 mm, and 20 mm for slab (I-15-0.66) specimen which shows a small variation in the sizing of the area of the damage zones as shown in Figure 19. It is fair to mention that a more accurate pattern and size of the damage zone area at both top and bottom faces of the slab is resulted using the finer mesh size of 10 mm in comparison to that of the coarser mesh of 15 mm and 20 mm.

ISSN 2349-4506
Impact Factor: 2.785

Global Journal of Engineering Science and Research Management

a. Simulation and test at bottom face of (I-10-0.59) slab specimen

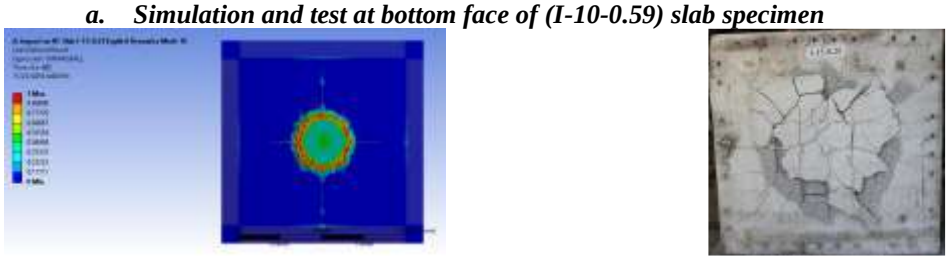

b. Simulation and test at bottom face of (I-15-0.25) slab specimen

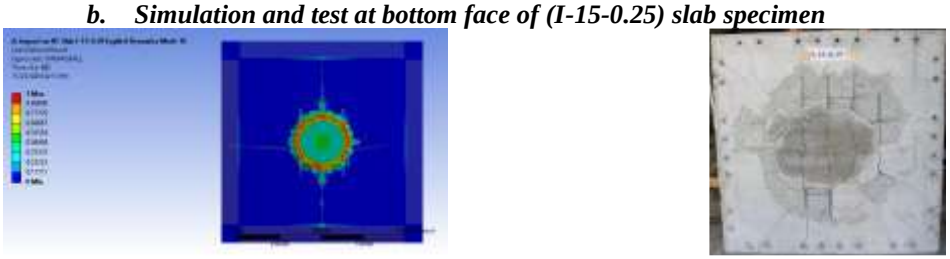

c. Simulation and test at bottom face of (I-15-0.39) slab specimen

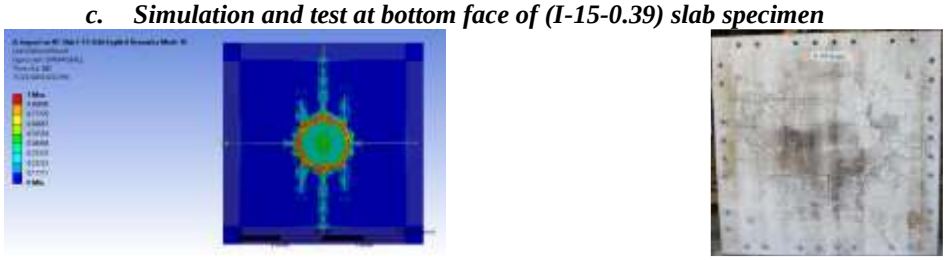

d. Simulation and test at bottom face of (I-15-0.66) slab specimen

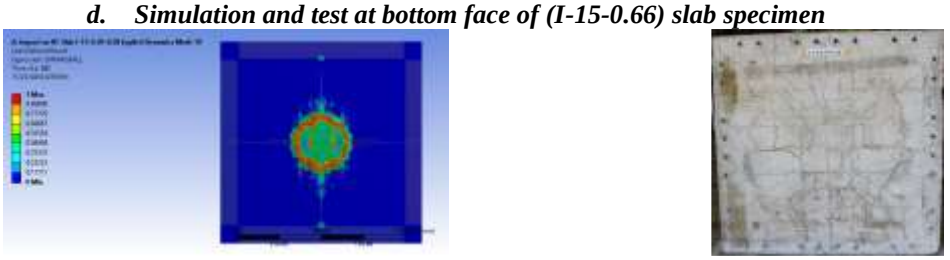

e. Simulation and test at bottom face of (I-15-0.39-0.28) slab specimen

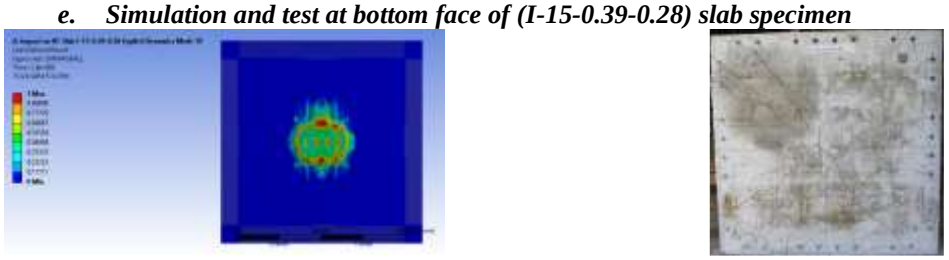

f. Simulation and test at bottom face of (I-15-0.39-0.56) slab specimen

Figure 18: Comparison of the damage and crack pattern resulted from the simulation with that of the tests at the bottom face of each of the slab specimens

ISSN 2349-4506
Impact Factor: 2.785

Global Journal of Engineering Science and Research Management

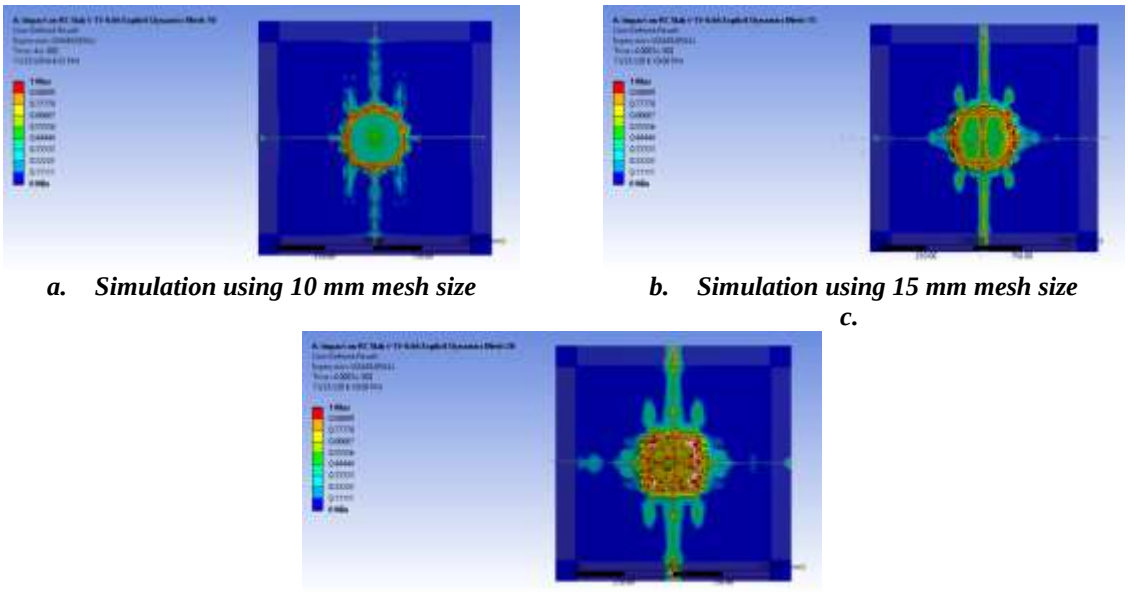

a. Simulation using 10 mm mesh size

b. Simulation using 15 mm mesh size

c.

d. Simulation using 20 mm mesh size

Figure 19: Comparison of the damage and crack pattern resulted from the simulation using three different mesh sizes at the bottom face of slab (I-15-0.66) specimen

CONCLUSIONS

Modeling of reinforced concrete slabs under impact loading using finite elements has been described. A presentation of the impact tests conducted on reinforced concrete slabs carried out by Xiao, Li [1] has been briefly described and a series of analyses using finite elements has been followed. A description and a comparison of the analysis results with those of the tests for impact force histories, displacement histories, crack patterns and damage have been presented. The following are the main drawn concluding remarks:

1. The crack patterns at the bottom face of all slab specimens was found to be in very good agreement when compared with those of the tests.
2. The damage zone at the impacted slab area is captured illustrating full perforation of the slabs without shear reinforcement compared with the slabs having shear reinforcements which in turn showed a remarkable penetration from observation of the tests. This damage zone diameter is found to be in very good matching with the tests. The cracking and damage extent to the slab bottom face shows a remarkable degree of scabbing similar to what has been observed in the tests.
3. Punching shear failure mode was observed for all the specimens that failed during the analysis similar to the experiment. Yielding of bottom reinforcement is observed at very early time of impact. The punching shear failure of specimens is featured by the fully formation of punching shear cone and its separation with nearby concrete, the residue strength of the slab is mainly contributed by top reinforcements whose yielding usually happen after punching shear failure.
4. Both longitudinal and transverse reinforcements are effective in enhancing the maximum strength of specimens which has been seen from the analysis and similar to the experiment. However, the benefits on slab's energy absorption capacity and impact resistance made by longitudinal reinforcement are limited comparing with shear reinforcement. The analysis as well as the experimental results show that the damage of slab under impact loading can be efficiently reduced by adding traditional shear stirrups.
5. Similar crack patterns, damage and failure process of specimen were found through the comparison between the analysis and the experiment. The punching shear failure of impacted slabs was very well predicted in the analysis.
6. It is then concluded that the suggested finite element model is valid to solve the reinforced concrete slab under impact problems.

ISSN 2349-4506
Impact Factor: 2.785

Global Journal of Engineering Science and Research Management

ACKNOWLEDGEMENTS

The authors would like to thank Prof. Dr. Thamir K. Mahmoud, Faculty Member of the Civil Engineering Department, College of Engineering, University of Baghdad for proposing the subject of this study. Special thanks to Dr. Hayder A. Al-Baghdadi, Faculty Member of the Civil Engineering Department, College of Engineering, University of Baghdad for his valuable comments and support.

REFERENCES

1. Xiao, Y., B. Li, and K. Fujikake, Experimental Study of Reinforced Concrete Slabs under Different Loading Rates. ACI Structural Journal, 2016. 113(1): p. 157.
2. Sangi, A.J., Reinforced concrete structures under impact loads. 2011, Heriot-Watt University.
3. Riedel, W., et al. Penetration of reinforced concrete by BETA-B-500 numerical analysis using a new macroscopic concrete model for hydrocodes. in Proceedings of the 9th International Symposium on the Effects of Munitions with Structures. 1999.
4. Riedel, W., Beton unter dynamischen Lasten: Meso-und makromechanische Modelle und ihre Parameter. 2000, EMI.
5. Riedel, W., N. Kawai, and K.-i. Kondo, Numerical assessment for impact strength measurements in concrete materials. International Journal of Impact Engineering, 2009. 36(2): p. 283-293.
6. Jones, N., Structural impact. 2011: Cambridge university press.
7. Peixinho, N. and A. Pinho, Study of viscoplasticity models for the impact behavior of high-strength steels. Journal of Computational and Nonlinear Dynamics, 2007. 2(2): p. 114-123
8. Fu, X. and D. Chung, Interface between steel rebar and concrete, studied by electromechanical pull-out testing. Composite Interfaces, 1998. 6(2): p. 81-92.